Internal Dynamics and Modular Peripheral Binding in Stimuli-Responsive 3 : 2 Host:Guest Complexes

Hang Yin, Roselyne Rosas, Stéphane Viel, Michel Giorgi, Valerie Monnier, Laurence Charles, Didier Siri, Didier Gigmes, Youssef Nassar, Floris Chevallier, et al.

How to cite: *Angew. Chem. Int. Ed.* **2024**, *63*, e202315985
doi.org/10.1002/anie.202315985

Host-Guest Systems

Internal Dynamics and Modular Peripheral Binding in Stimuli-Responsive 3:2 Host:Guest Complexes

Hang Yin, Roselyne Rosas, Stéphane Viel, Michel Giorgi, Valerie Monnier, Laurence Charles, Didier Siri, Didier Gigmes, Youssef Nassar, Floris Chevallier, Christophe Bucher, Ruibing Wang,* Anthony Kermagoret,* and David Bardelang**

Abstract: Now that the chemistry of 1:1 host:guest complexes is well-established, it is surprising to note that higher stoichiometry (oligomeric) complexes, especially those with excess host, remain largely unexplored. Yet, proteins tend to oligomerize, affording new functions for cell machinery. Here, we show that cucurbit[*n*]uril (CB-[*n*]) macrocycles combined with symmetric, linear di-viologens form unusual 3:2 host:guest complexes exhibiting remarkable dynamic properties, host self-sorting, and external ring-translocation. These results highlight the structural tunability of cucurbit[8]uril (CB[8]) based 3:2 host:guest complexes in water and their responsiveness toward several stimuli (chemicals, pH, redox).

[*] H. Yin, Prof. R. Wang
State Key Laboratory of Quality Research in Chinese Medicine, Institute of Chinese Medical Sciences, University of Macau
Taipa, Macau (China)
E-mail: rwang@um.edu.mo

R. Rosas, Dr. M. Giorgi, Dr. V. Monnier
Aix Marseille Univ, CNRS, Centrale Marseille, FSCM, Spectropole
Marseille (France)

Prof. S. Viel, Prof. L. Charles, Prof. D. Siri, Dr. D. Gigmes, Dr. D. Bardelang
Aix Marseille Univ, CNRS, ICR, AMUtech
Marseille (France)
E-mail: david.bardelang@univ-amu.fr

Prof. S. Viel
Institut Universitaire de France
75005 Paris (France)

Y. Nassar, Dr. F. Chevallier, Dr. C. Bucher
Univ Lyon, Ens de Lyon, CNRS UMR 5182, Laboratoire de Chimie
69342 Lyon (France)
E-mail: christophe.bucher@ens-lyon.fr

Dr. A. Kermagoret
Aix Marseille Univ, CNRS, CINaM, AMUtech
Marseille (France)
E-mail: anthony.kermagoret@univ-amu.fr

Introduction

One of the most fascinating aspects of proteins is their ability to self-assemble into well-defined architectures, thereby creating new functions.[1] For example, nicotinic acetylcholine receptors are a class of ionic channels for which most neuronal subtypes comprise α and β subunits arranged in 2:3 or 3:2 stoichiometry.[2] The oligomeric structure of $\alpha_2\beta_3$ or $\alpha_3\beta_2$ clusters is crucial for these assemblies to function as ligand-gated ion channels.[3] In supramolecular chemistry, most research efforts have so far focused on low-stoichiometry host:guest complexes.[4] However, higher stoichiometry supramolecular assemblies are receiving increasing attention,[5] motivated by the prospects of discovering new properties, specific of these assemblies at the forefront of science (i.e. in optical, electronic or biological domains),[6] or yet to discover. Most of the work currently carried out in this field aims at modulating the size and diversity of metal-organic cages,[7] or to form assemblies of precise size and shape from relevant host and guest molecules.[8] In particular, several works have taken advantage of the outstanding recognition properties of cucurbit-[*n*]urils (CB[*n*], Scheme 1) host molecules ($K_a = 10^{2-17}$ M^{-1} in water),[9] to explore homo- and hetero-oligomerization.[10]

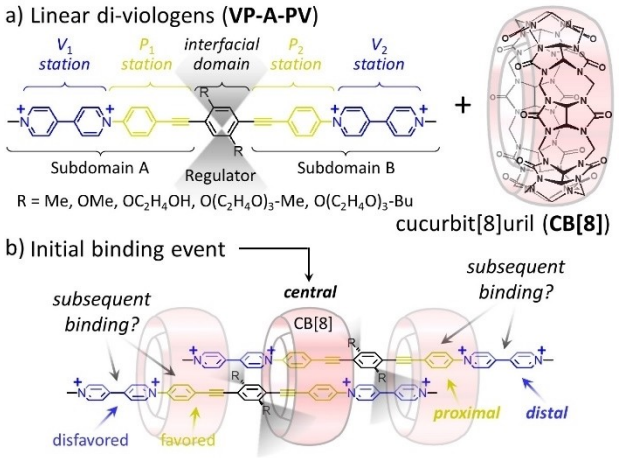

Scheme 1. (a) Structures of guest molecules and macrocyclic host used in this work affording (b) well-defined 3:2 host:guest complexes (the blurred grey areas schematically indicate conformational flexibility or steric hindrance.

However, the control of successive binding events remains challenging,[11] a major limitation being the difficulty to avoid supramolecular polymerization.[12] Among the CB[*n*] discrete assemblies reported so far, one can distinguish those involving an even number of molecules from those involving an odd number. While "even assemblies" are frequently observed,[10a] "odd clusters" remain rare, with few examples of 3:2 host:guest complexes.[13] Besides, no rationale has been proposed to understand and predict their formation.

We show that CB[8] can form stable 1:2 intermediates with linear diviologens.[14] This results in a desymmetrization of the two guest molecules providing binding sites for two additional CB[8]. This assembly has been exploited to access several well-defined 3:2 complexes whose properties are discussed hereafter.

Results and Discussion

Syntheses

The guest molecules incorporate two pairs of stations, noted P_i and V_i, with potential affinity for CB[8].[15] The two types of stations are symmetry related by a C_2 symmetry axis passing through the central benzene ring (Scheme 1). Different substituents (R groups) were introduced on the central aryl spacer of the Viologen-Phenylene-Aryl-Phenylene-Viologen guests (**VP-A-PV**) to gradually impact CB[*n*] binding and probe the stability of 3:2 complexes. **VP-A-PV** derivatives were prepared from selected precursors by Sonogashira couplings and Zincke reactions (Supporting Information, Figures S1 to S23).

Common structural motif: 1:2 inclusion complexes

The inclusion of **VP-A-PV** in CB[*n*] ($n=7$, 8) was investigated by ^{1}H NMR spectroscopy in D_2O. The addition of CB[7] to guest solutions led to the observation of 2:1 host:guest complexes, the two CB[7] always sitting on V_i stations of each guest (Figures S24 to S31). The stoichiometry was confirmed by ITC for **VP-A-PV**-$(OMe)_2$ and allowed to estimate a binding constant $K_a = 7.2\times10^5\ M^{-1}$, identical for each site, Figure S32).[16] Titrations of CB[8] with **VP-A-PV** in D_2O (Figures S33 to S37) consistently led to the observation of stable 1:2 host:guest complexes (Figure 1b and Figures S33 to S51). The addition of 0.5 molar equivalent of CB[8] led to a splitting of ^{1}H NMR signals assigned to P_i stations, the large upfield shift experienced by a single set of signals ($<\Delta\delta Hf1,g1> \approx -0.90$ ppm) suggesting that half of the P_i stations are included in CB[8]. The formation of 1:2 complexes involving the CB[8] inclusion of two phenylene stations, each belonging to one guest molecule was confirmed by single crystal X-ray diffraction (CCDC 2182217, Figure 2).[17] The two included phenyl rings are tilted by 41° with respect to the mean plan of the guest molecules and they are separated by 3.99 Å. The position of attached protons is special and will be discussed later.

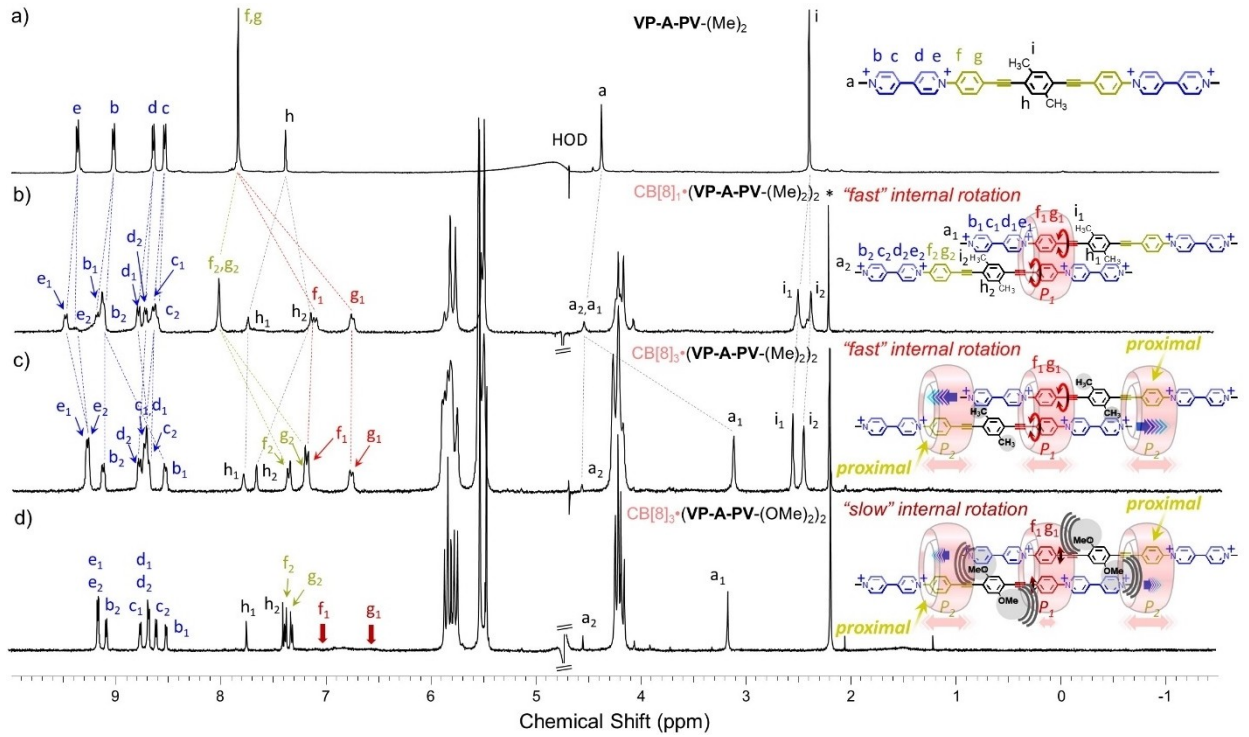

Figure 1. ^{1}H NMR spectra (300 MHz, 298 K, D_2O) of (a) **VP-A-PV**-$(Me)_2$, CB[8] addition being featured by formation of (b) a 1:2 complex ca. 0.5 equiv. CB[8], and (c) a 3:2 complex ca.1.5 equiv. of CB[8]. (d) 3:2 complex from **VP-A-PV**-$(OMe)_2$ with CB[8] (*: acetone, watergate sequence used to improve signal-to-noise ratios, for concentrations see the Supporting Information).

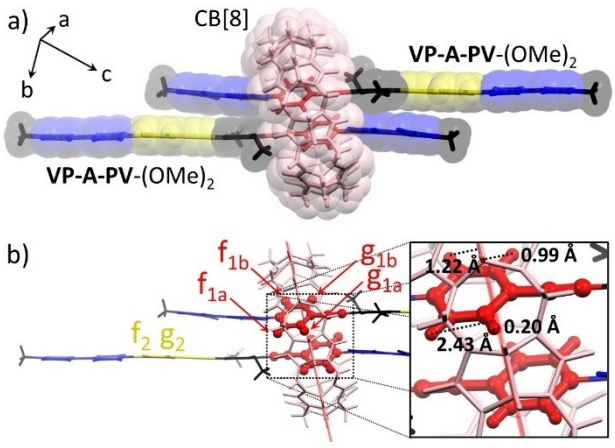

Figure 2. (a) Structure of the 1:2 CB[8]$_1$•(**VP-A-PV**-(OMe)$_2$)$_2$ complex determined by single-crystal X-ray diffraction (other molecules removed for clarity). (b) Focus on the position (see inset) of inner cavity protons f_{1a}, f_{1b}, g_{1a}, g_{1b} toward the mean plane of CB[8] (in light red; see text).

3:2 complexes with proximal peripheral binding

^{1}H NMR spectra recorded after addition of one equiv. of CB[8] to aqueous solutions of **VP-A-PV** guests carrying small R groups (R = Me, OMe, OC_2H_4OH) proved difficult to analyze. Observation of complex spectra was attributed to the formation of unsymmetrical 2:2 complexes following the threading of an additional CB[8] on an "external" station available on the initial 1:2 complexes (Figures S33 to S37). Further changes were observed in the ^{1}H NMR spectra as the host/guest ratio gradually increased, reaching a final and stable state after the addition of ~1.5 equiv. of CB[8]. ^{1}H NMR spectra recorded at this stage were consistent with the formation of "compact" CB[8]$_3$•(**VP-A-PV**)$_2$ complexes, with one CB[8] in central position, and two more threaded on *proximal* outer phenylene stations (Figure 1c, 1d and Figures S53 to S61). This attribution relies on detailed analyses of NMR data, including the consistent observation of (i) two sets of signals at ≈8.5–9.2 ppm and ≈8.6–9.2 ppm corresponding to "uncomplexed" viologens, (ii) two sets of signals at ≈6.6–7.2 ppm and ≈7.2–7.4 ppm assigned to complexed phenylenes (P_1 and P_2) in different chemical environments, (iii) the stoichiometry, in line with the relative integration of host and guest signals (1.5 to 1), and (iv) the large upfield shift experienced by proton a_1 at ≈3.1 ppm ($\Delta\delta \approx -1.1$ ppm) assigned to two CB[8]-included methyl groups. This result is a strong evidence for a simultaneous inclusion of two viologen *methyl* groups, the *phenylene* stations of neighboring guest molecules (P_2) being also included in a CB[8]. This additional *external* binding could explain the formation of these 3:2 complexes, preventing inclusion of more guests and the formation of polymers.[12a,b] DOSY experiments recorded on solutions of **VP-A-PV** (small R groups) containing ≥1.5 molar equiv. of CB[8] showed one set of aligned signals in line with a single complex exhibiting a substantially lower diffusion coefficient ($D = [1.48–1.61]\times10^{-10}$ m^2.s^{-1}, Figures S62 to S64)[18] than for previously reported CB[8] 2:2 complexes [1.60–2.24]$\times10^{-10}$ m^2.s^{-1}).[10a]

Our work also revealed that the bulkiness of R substituents of the central aryl ring (**A** unit in **VP-A-PV**) has a strong impact on the association mode, and on the dynamics of exchange processes in solution. This effect was initially brought to light by comparing the spectra of **VP-A-PV**-(Me)$_2$ and **VP-A-PV**-(OMe)$_2$ solutions with 1.5 molar equiv. of CB[8]. The ^{1}H NMR spectrum of the 3:2 complex formed with **VP-A-PV**-(Me)$_2$ showed two well-resolved signals at 6.75 and 7.18 ppm (f1 and g1 in Figure 1c) assigned to P_1 stations in CB[8], while the one recorded with **VP-A-PV**-(OMe)$_2$ showed no trace of these signals which seem to have disappeared (Figure 1d, similar result for **VP-A-PV**-(OC_2H_4OH)$_2$ Figure S59). This result was difficult to understand due to the small structural difference between **VP-A-PV**-(Me)$_2$ and **VP-A-PV**-(OMe)$_2$, but we realized that the bulkier methoxy groups could have sandwiched the central CB[8], dramatically limiting its internal translation (Figure 1d). The two **VP-A-PV**-(OMe)$_2$ molecules could thus have less freedom to accommodate rotational changes of the two included P_1 stations. Raising temperature enabled to recover the missing signals (Figure 3a and Figure S65) while decreasing temperature showed a splitting of f_1 and g_1 signals into $f_{1a}+f_{1b}$ and $g_{1a}+g_{1b}$, respectively. Coalescence of the signals around $T_C = 313$ K was assigned to hindered rotation of included P_1 stations below T_C and to retrieved rotation above T_C.[19] Careful inspection of the X-ray structure (Figure 2b) showed the two phenylene units in red, symmetry-related by an inversion centre, each of them possessing four non-equivalent protons (f_{1a}, f_{1b}, g_{1a}, g_{1b}). While f_{1a} is close to carbonyl portals in line with a deshielded signal (Figure 3a, 278 K), g_{1a} is at only 0.2 Å from the cavity mean plane, consistent with the largest upfield shift (Figure 3a, 278 K).[14–16,18] Instead, f_{1b} and g_{1b} at 1.22 and 0.99 Å respectively from the cavity mean plane are expected to be in a similar environment and resonate at similar frequencies as observed in NMR (Figure 3a, bottom).

Simulations of the 800 MHz ^{1}H NMR spectra at different temperatures allowed us to estimate the rate of exchange between the P_1 intra cavity protons (f1a↔f1b, g1a↔g1b) of CB[8]$_3$•(**VP-A-PV**-(OMe)$_2$)$_2$ ($k = 50–4500$ s^{-1}, Figure 3a, inset and Supporting Information). Building an Eyring plot allowed us to estimate the activation energy corresponding to the rotation of P_1 in the 3:2 complex $\Delta G^{\ddagger}$ (298 K) = 14.2 kcal.mol^{-1} which is mainly (>89 %) enthalpic ($\Delta H^{\ddagger}$ = 12.7 kcal.mol^{-1}). This energetic cost likely reflects the energy needed to reach a transition state in which the two included phenylenes are perpendicular. It may be due to (i) internal guest strain to accommodate the edge-to-face P_1-P_1 conformations, (ii) unfavourable deformations of the CB[8] cavity to allow for such movements or (iii) unfavourable guest translation (methoxy steric clash) toward the centre of the 3:2 complex to place the less sterically demanding alkyne bond near the centre of CB[8], and enable the other P_1 to rotate (Figure 3b). Molecular dynamic studies (Figure 3b) revealed that the CB[8]$_3$•(**VP-A-PV**-(OMe)$_2$)$_2$ complexes are stable over 100 ns in water, with two peripheral CB[8] on P_2 stations, each of them co-including one

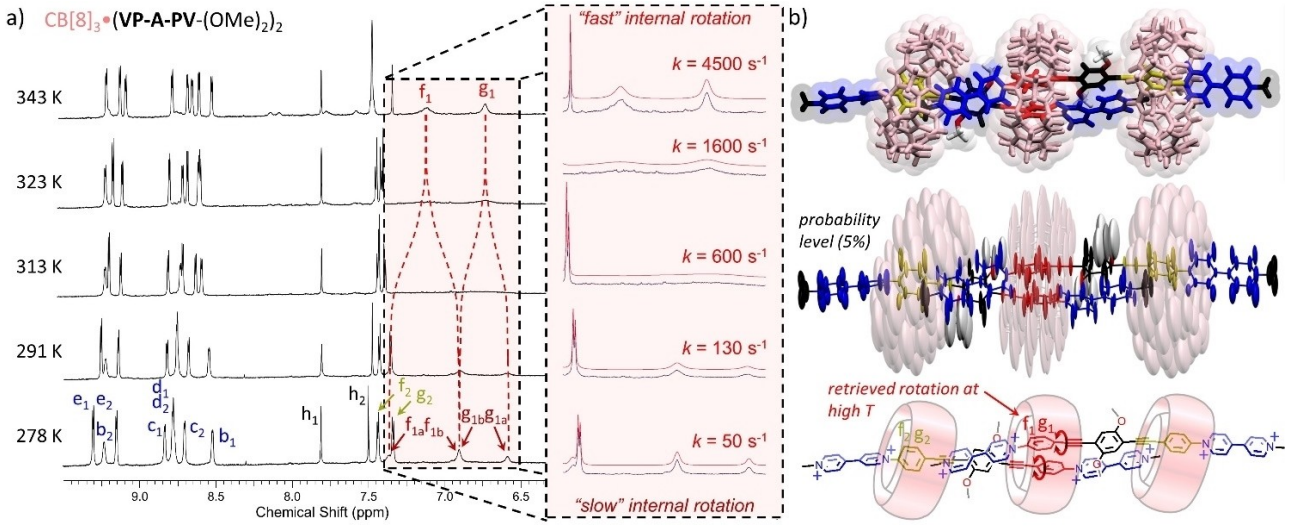

Figure 3. (a) Aromatic region of 800 MHz variable-temperature ^{1}H NMR spectra of CB[8]$_3$•(**VP-A-PV**-(OMe)$_2$)$_2$ (0.25 mM in D_2O) with an enlargement (inset) of the region corresponding to protons f_{1a}, f_{1b}, g_{1a}, g_{1b} and coalescence of their signals upon temperature increase. (b) Top: representative structure of the molecular dynamics in water; centre: ellipsoid representation showing weighted contributions of local movements of each atom around their mean position; bottom: schematic representation of the structure with the studied rotations shown in red.

neighbouring methyl-pyridinium in good agreement with NMR data discussed above. In the proposed 3:2 complexes, the central CB[8] are much less mobile than the two peripheral CB[8] (Figure 3b), the methoxy groups behaving as *supramolecular wedges*, "blocking" the central CB[8] on the P_1-P_1 stations and preventing guest translation (distance between the central phenylene of each guest = 13.2 ± 0.4 Å, Figure S66) and probably P_1 station rotation. This effect was confirmed by comparing the ^{1}H NMR spectra recorded for different 1:2 complexes and by showing that the signals of protons H_{f1} and H_{g1} are sharp for **VP-A-PV**-(Me)$_2$, broad for **VP-A-PV**-(OMe)$_2$ and almost disappeared for **VP-A-PV**-(OC$_2$H$_4$OH)$_2$ (Figure S41, S44, S47). The two peripheral CB[8] are also involved in a rigidification of the 3:2 complexes, likely contributing to the hampered rotation of the P_1 stations, as revealed by the signals of protons H_{f1} and H_{g1} that are broad but still clearly visible in the 1:2 complex formed with **VP-A-PV**-(OMe)$_2$ (Figure S44), but virtually not observed in the corresponding 3:2 complex (Figure 1d). The two peripheral CB[8] thus behave as *supramolecular clamps*,[10b,20] remotely restricting the rotation rate of both phenylenes included in the central CB[8] ring, most probably through a rigidification of the complex impeding the relative translation of hosts and guests. Of note, peculiar internal dynamics was observed previously for CB[8] based 2:2 complexes but relying on different mechanisms.[20a] As a matter of fact, this is the first example to our knowledge of artificial mechanical coupling between translational and rotational motions within large water-soluble supramolecular complexes (molecular weight >5300 Da approaching that of small proteins). By exploring how the length of the side-arms (R groups of **VP-A-PV**, Scheme 1) impacts the formation of these 3:2 complexes, we found that appropriate R groups can stabilize another kind of 3:2 complexes with two peripheral CB[8] rings located on distal stations.

3:2 complexes with distal peripheral binding

^{1}H NMR titrations with **VP-A-PV**-(O(C$_2$H$_4$O)$_3$CH$_3$)$_2$ and CB[8] (Figure S36) showed the formation of a final stable 2:1 complex in the presence of excess host, in equilibrium with a small amount of a 3:2 complex (Figures S67 and S68). However, with side-arms carrying an additional hydrophobic butyl group, NMR studies showed the formation of a new 3:2 complex (Figure 4a) featured by a different structure. ^{1}H NMR titrations of a solution of **VP-A-PV**-(O(C$_2$H$_4$O)$_3$-Bu)$_2$ with CB[8] (Figure S37) first showed the occurrence of the expected 1:2 complex at 0.5 equiv. of host (Figure 4b and S49, confirmed by DOSY, Figure S69).

However, with two molar equiv. of CB[8], new sets of resonances were observed (Figure 4c) assigned to a previously unobserved kind of 3:2 host:guest complex (supported by integration and DOSY, Figures S69 to S75). This new complex in which a central CB[8] still binds two P_1 stations (broad signals in the 6.7–7.2 ppm region), now leaves the two P_2 stations unoccupied. The ^{1}H NMR spectrum of that species also exhibits different sets of signals for "free" and "complexed" viologens. These results are in stark contrast with ^{1}H NMR spectra of CB[8]$_3$•(**VP-A-PV**-(R)$_2$)$_2$ (R = small alkyl or alkoxide groups) discussed above which showed that the *Pi* stations are complexed while *Vi* units are all free. Another major difference in the ^{1}H NMR spectrum shown in Figure 4c compared to previous spectra, is the presence of strongly shielded signals at 7.70 and 7.85 ppm corresponding to viologen protons c2 and d2 included in CB[8].[14–16,18] Taken together, these data support the formation of a new 3:2 complex featuring a specific

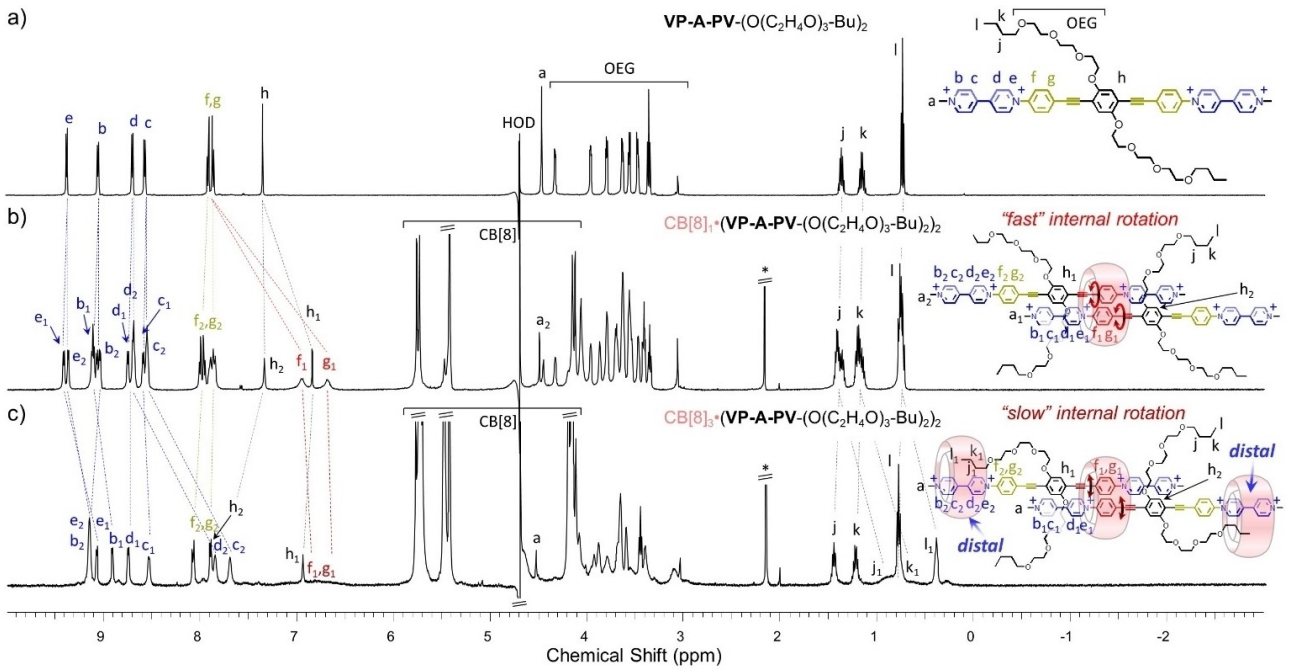

Figure 4. ^{1}H NMR spectra (500 MHz, 298 K, D_2O) of (a) **VP-A-PV**-$(O(C_2H_4O)_3\text{-}Bu)_2$ and (b and c) with increasing amounts of CB[8] and proposed complexes (*: acetone, watergate sequence used to improve signal-to-noise ratios; for concentrations see the Supporting Information).

binding mode in which (i) both central P_1 stations are inserted within the cavity of one CB[8] ring, and (ii) two peripheral CB[8] rings are located on *distal* viologen stations. Another striking feature of the proposed complex is the peripheral co-inclusion of butyl groups with viologens in the outer CB[8],[21] providing a reasonable explanation for the translocation of peripheral CB[8] from *proximal* to *distal* stations. This insertion of half the number of butyl chains in CB[8] is demonstrated by a splitting of all signals between 0 and 2 ppm (Figure 4c) into two sets of resonances (same relative integration), one with sharp signals assigned to "free" butyl groups and the other with broad upfield shifted signals assigned to "complexed" butyl groups. The signals of H_{f1} and H_{g1} are barely distinguishable at room temperature due to restrictions in rotational movements of P_1 stations in the central CB[8], but again sample heating enabled P_1 stations to recover some rotational freedom as proved by the intense signals of Hf1 and Hg1 at 343 K (Figure 5a and Figure S76). Simulations of NMR spectra in the 278–343 K range allowed us to determine the rotational rate constants corresponding to the exchange of protons H_{f1} and H_{g1} between sites "a" and "b" (70—7700 s^{-1}, Figure 5a). Use of the Eyring equation then enabled us to estimate the activation energy corresponding to the rotation of P_1 stations in the central CB[8], $\Delta G^{\ddagger}$ (298 K) = 13.9 kcal.mol^{-1}, being again mainly enthalpic ($\Delta H^{\ddagger}$ = 12.2 kcal.mol^{-1}). Molecular dynamics studies showed that the 3:2 complex $CB[8]_3^{\bullet}$ **(VP-A-PV**-$(O(C_2H_4O)_3\text{-}Bu)_2)_2$ is stable for at least 100 ns in water (Figure 5b). The central CB[8] was also found to be less mobile than the others, likely due to the two pairs of OEG chains flanked near its two carbonyl rims. This form of steric hindrance could decrease the mobility of the CB[8] rings, thereby impeding guest translation (distance between the central phenylene of each guest = 12.8 ± 0.4 Å, Figure S77) and probably rotation of P_2 stations. Finally, co-inclusion of the butyl and viologen units in the two *distal* CB[8] was confirmed, resulting in another peripheral *rigidification* but this time on external viologens. Thus, changing the length and nature of the side-arms of **VP-A-PV** guests made it possible to shift the position of both peripheral CB[8] rings from *proximal* to *distal* stations.

3:2 complexes with CB[8] and CB[7]

Fostered by the possibility to change the outer binding from P_i to V_j stations, we wondered whether CB[7] could also occupy the peripheral V_i stations of the 1:2 CB[8]:**VP-A-PV** complexes. The NMR spectrum recorded for a 2:1:2 mixture of CB[7], CB[8] and **VP-A-PV**-$(OMe)_2$ in D_2O (Figure 6a and Figure S78), was different from those corresponding to the $CB[8]_3^{\bullet}$**(VP-A-PV**-$(OMe)_2)_2$ or $CB[7]_2^{\bullet}$**VP-A-PV**-$(OMe)_2$ complexes.

COSY NMR spectra recorded in these conditions (Figure S79) revealed that ^{1}H NMR spectra include two sets of resonances assigned to the phenylene stations (not included and included in CB[8]) and two sets of resonances assigned to viologen stations (likewise not included and included in CB[7]). Of note, the large upfield shifts of proton signals c2 and d2 near 7 ppm ($|\Delta\delta| > 1.2$ ppm) are diagnostics of CB[7] complexation on viologens (see NMR of $CB[7]_2^{\bullet}$**VP-A-PV**-$(OMe)_2$, Figure S27). These data are thus consistent with a new supramolecular complex: $CB[8]_1^{\bullet}CB[7]_2^{\bullet}$**(VP-A-PV**-$(OMe)_2)_2$ wherein the CB[7] and CB[8] rings have been

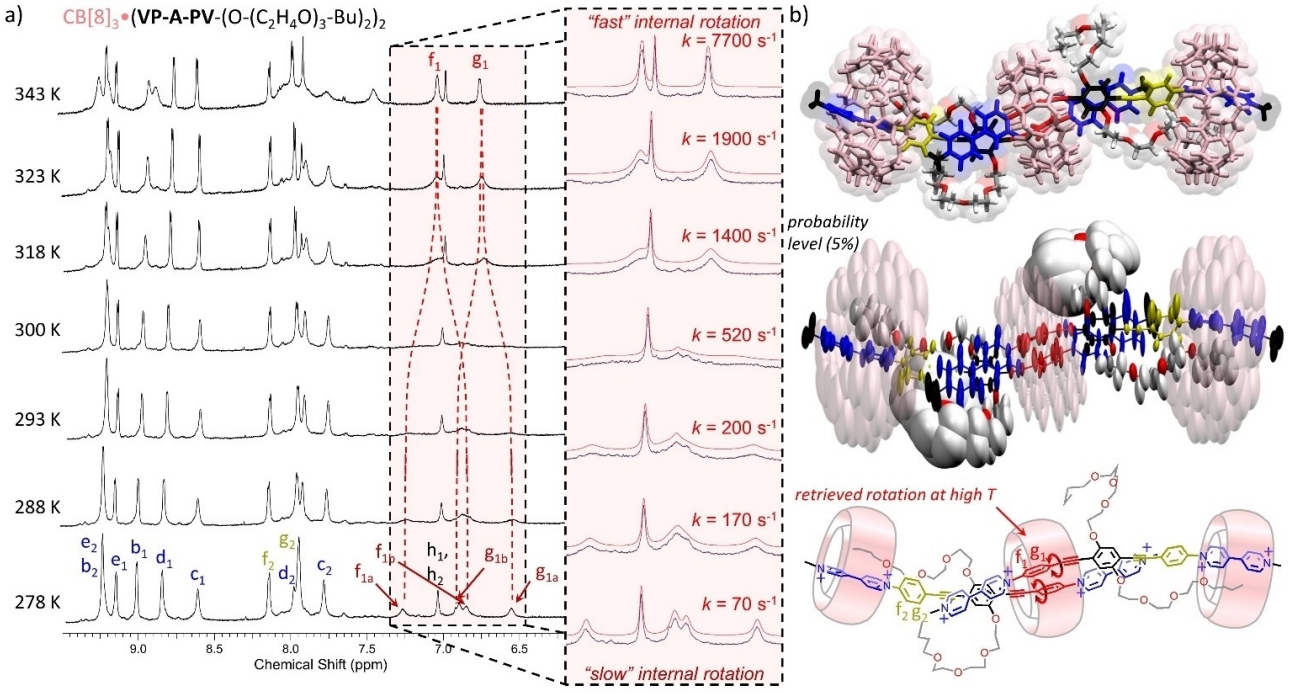

Figure 5. (a) Aromatic region of 800 MHz variable-temperature ^{1}H NMR spectra of CB[8]$_3$•(**VP-A-PV**-(O-(C$_2$H$_4$O)$_3$-Bu)$_2$)$_2$ (0.26 mM) in D$_2$O with an enlargement (inset) of the region corresponding to protons f_{1a}, f_{1b}, g_{1a}, g_{1b} and coalescence of their signals upon temperature increase. (b) Top: representative structure of molecular dynamics in water; center: ellipsoid representation showing weighted contributions of local movements of each atom around their mean position; bottom: schematic representation of the structure with the studied rotations shown in red.

sorted and positioned on specific stations.[11a,15a, 22] Similar results were obtained with **VP-A-PV**-(Me)$_2$ (Figures S80 and S81). This illustrates well the modularity that can be achieved in cucurbituril host:guest 3:2 assemblies.

3:2 complexes with selective ring translocation

The ability of CB[8] to promote the formation of charge transfer (CT) complexes between viologen-based acceptors and naphthalene-based donors has been widely exploited in supramolecular chemistry.[10a,23] We have thus checked whether such complexation could be used to promote a translocation of both peripheral CB[8] on distal (V_i) stations.[24] These studies consisted in monitoring the changes in the ^{1}H NMR spectra of CB[8]$_3$•(**VP-A-PV**-(R)$_2$)$_2$ (R = Me, OMe or OC$_2$H$_4$OH) upon addition of 2,6-dihydroxynaphthalene (26-DN).[23–24] As expected, the addition of 6.6 molar equivalents of 26-DN to a solution of CB[8]$_3$• (**VP-A-PV**-(Me)$_2$)$_2$ led to the disappearance of the initial spectrum in favor of new signals that could be assigned to the CT complex shown in Figure 6b (see also Figure S82). COSY NMR spectra (Figure S83) proved useful to unambiguously assign all those resonances and to show that the f_1/g_1 and f_2/g_2 signals correspond to hydrogen atoms of different phenylene stations (P_i) located either inside or outside a CB[8] ring, respectively. Two different sets of signals were similarly attributed to viologen units locked in different chemical environments: i) a first set assigned to $H_{b1\text{-}e1}$, only slightly shifted compared to the signals of a free viologen and ii) a second set of signals including strongly shielded resonances of c2 and d2 protons at ≈6.9 ppm ($|\Delta\delta| > 1.7$ ppm) assigned to the formation of a CB[8]-stabilized viologen-naphthalene CT complex. Therefore, the addition of 26-DN, used here as a chemical stimulus, allowed a peripheral translocation of both CB[8] rings, from *proximal* to *distal* stations of the in situ prepared 3:2 host:guest complex. Finally, when CB[8] and 2,6-DN were used in large excess, the 3:2:2 donor-acceptor complex shown in Figure 6b could be transformed into the 2:1:2 complex CB[8]$_2$•(**VP-A-PV**-(Me)$_2$)$_1$•(2,6-DN)$_2$ (Figure S84).

pH-responsive 3:2 complexes: interconversion between 3:2 and 2:2 complexes

The pyridine-pyridinium motif (**PyP$^+$**) has attracted increased attention in recent years as a building block for supramolecular assemblies due to its ability to undergo homodimerization in the cavity of CB[8].[25] We therefore turned our attention to the self-assembly properties of the unmethylated analogue **PyP$^+$-A-P$^+$Py**-(OC$_2$H$_4$OH)$_2$, incorporating two pyridine end-groups (Figure 6c, synthesis in Supporting Information). Its ability to self-assemble in the presence of CB[8] and to undergo structural modifications by pH changes was revealed by NMR spectroscopy (Figure 6 bottom and Figure S85). The ^{1}H NMR spectrum recorded in D$_2$O after addition of 2 molar equiv. of CB[8] is shown in Figure 6d. The upfield shifted signals of proton c (confirmed by COSY NMR, Figure S86) suggests that CB[8] rings are

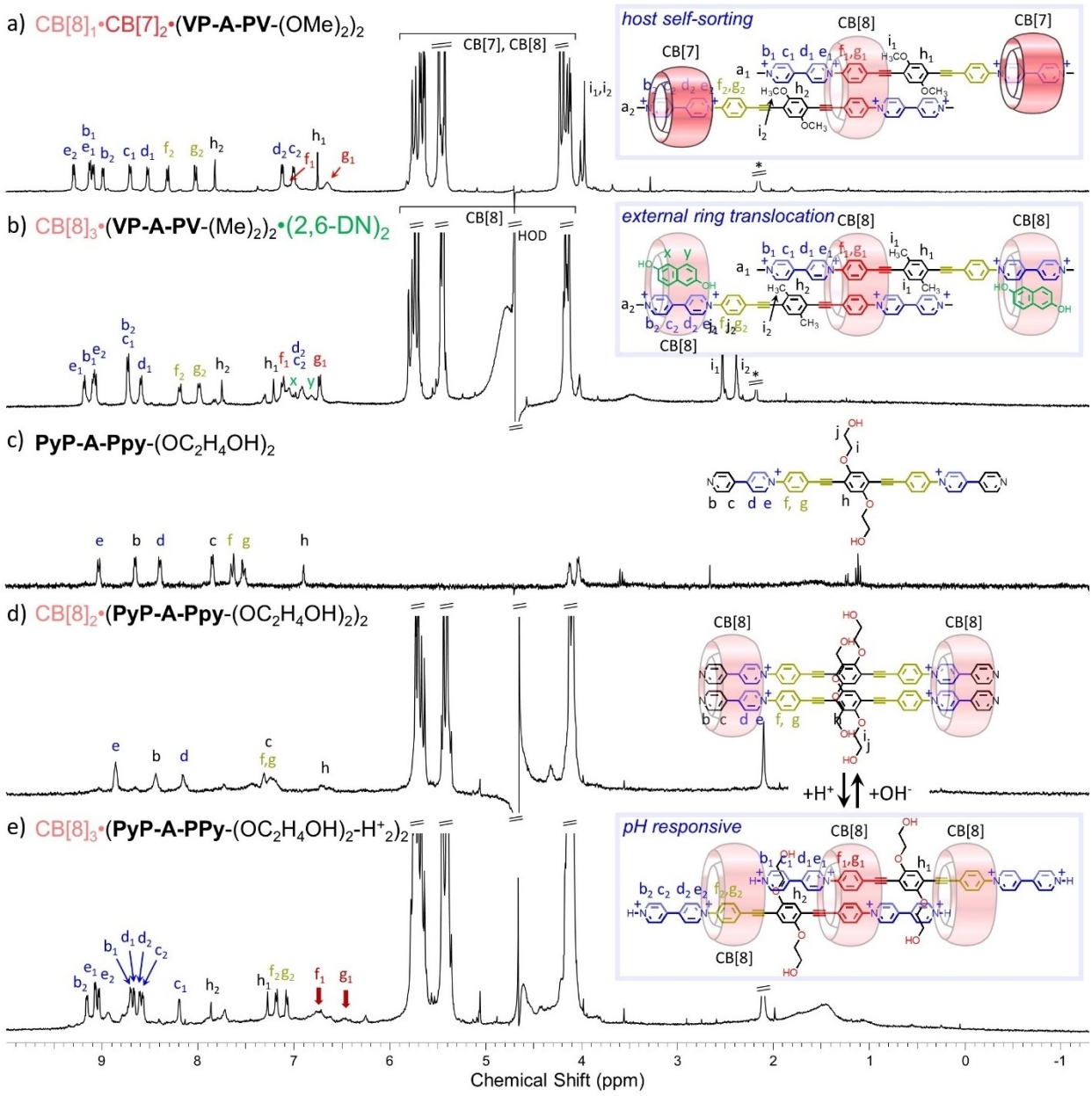

Figure 6. ^{1}H NMR spectra (300 MHz, 298 K, D_2O) of (a) the sorted hosts CB[7]$_2$•CB[8]$_1$•(**VP-A-PV**-(OMe)$_2$)$_2$ (0.5 mM) complex, and (b) the CB[8]$_3$•26-DN$_2$•(**VP-A-PV**-(Me)$_2$)$_2$ complex (0.15 mM * is for acetone used as an internal reference; a watergate sequence was used to improve signal-to-noise ratios). 26-ND was used to translocate two peripheral CB[8] rings on the periphery of 3 : 2 complexes from proximal to distal stations. ^{1}H NMR spectra (500 MHz, 298 K, D_2O) of (c) **PyP-A-PPy**-(OC$_2$H$_4$OH)$_2$ alone (0.25 mM), (d) with 2 equiv. of CB[8] and (e) after the addition of 10 more equiv. of TFA.

positioned around the **PyP$^+$** stations. However, while the resonances of CB[8] remain sharp, broad signals were observed in the aromatic region and could be due to ring shuttling between the stacked **PyP$^+$-PyP$^+$** units and the stacked ***P-P*** stations. DOSY NMR confirmed the presence of a single species featured by a diffusion coefficient $D = 1.79\times10^{-10}$ m^2.s^{-1}, in line with a discrete CB[8] 2 : 2 complex (Figure S87). This diffusion coefficient was indeed found to be smaller than that of the guest alone ($D = 2.28\times10^{-10}$ m^2.s^{-1}) but larger than those of CB[8]-based 3 : 2 complexes ($D = [1.48–1.61]\times10^{-10}$ m^2.s^{-1}). More interestingly, we found that a protonation of both terminal pyridines, readily achieved by addition of 10 molar equiv. of TFA, resulted in a markedly different spectrum with sharp lines (Figure 6e and Figure S88) that could be assigned to the host:guest 3 : 2 complex shown in Figure 6e (excess host was initially present, see COSY NMR, Figure S89). In particular, the observation of two sets of signals for viologens (b1-e1 and b2-e2) in a region corresponding to "free" viologens, and two sets of signals as well, broad for f_1, g_1 and sharp for f_2, g_2, both corresponding to included phenylenes strongly support this assignment. The measured diffusion coefficient

$D = 1.54\times10^{-10}$ m^2.s^{-1} (Figure S90) moreover happened to fall in the expected domain for a CB[8] 3:2 complex. Finally, a back conversion of this 3:2 species into the initial 2:2 complex could be achieved by addition of $NaHCO_3$ leading to a deprotonation of the terminal pyridinium and to a sliding motion of both **PyP-A-PPy**-$(OC_2H_4OH)_2$ guest molecules coming along with the ejection of one CB[8] host. The addition of acid or base thus proved to be an efficient way to control the stoichiometry of the self-assembled complexes generated in situ from **PyP-A-PPy**-$(OC_2H_4OH)_2$ and CB[8].

Reduction of the 3:2 complexes: toward paramagnetic 2:2 complexes

The 3:2 complex obtained from **V^{2+}P-A-PV^{2+}**-$(OMe)_2$ was characterized by cyclic voltammetry (CV) measurements. The CV curves recorded in water (+LiCl) at a vitreous carbon working electrode before and after addition of 1.5 molar equiv. of CB[8] are shown in Figure 7. The stability of the discussed inclusion complexes in the conditions of CV measurements was confirmed by NMR measurements carried out in the presence of electrolyte.

As expected, the free ligand undergoes two successive one electron reduction (1e$^-$/viologen) yielding the bis-cation radical **V$^{+\bullet}$P-A-PV$^{+\bullet}$**-$(OMe)_2$ and the neutral analogue **V^{0}P-A-PV^0**-$(OMe)_2$ (black line in Figure 7). The Gaussian shape of the second reduction wave observed at $E_p = -0.715$ V and of all the oxidation waves observed on the return scan are clearly demonstrating the physisorption of the reduced forms at the glassy carbon electrode surface, which makes sense given the strong organic character of the molecule. With respect to the first reduction wave, we found that the adsorption of **V$^{+\bullet}$P-A-PV$^{+\bullet}$**-$(OMe)_2$ could not be avoided by increasing the scan rate, as evidenced by the observation of intense anodic redissolution peaks at all studied scan rates (Figure S91). This behavior contrasts with the standard diffusion-controlled response observed in organic electrolytes (see Figure S92) where all redox states of the molecule where found to be perfectly soluble. In situ formation of the 3:2 inclusion complex CB[8]$_3^{\bullet}$(**V^{2+}P-A-PV^{2+}**-$(OMe)_2)_2$ was first revealed by a strong decrease in the intensity of all the reduction waves (blue curve in Figure 7), which is consistent with an increase in the size of the species formed in solution leading to a decrease in their diffusional mobility. It was also further revealed by the disappearance of the Gaussian-shaped re-dissolution peaks, suggesting that the formation of CB[8]$_3^{\bullet}$(**V^{2+}P-A-PV^{2+}**-$(OMe)_2)_2$ in solution prevents the adsorption of the bisradical **V$^{+\bullet}$P-A-PV$^{+\bullet}$**-$(OMe)_2$ and its quinonic form **V^{0}P-A-PV^0**-$(OMe)_2$. Complexation was also found to result in a shift of both reduction waves towards more negative values, from $E_{p1} = -0.285$ V and $E_{p2} = -0.715$ V measured for the free guest, to $E_{p1} = -0.340$ V and $E_{p2} = -1.065$ V for the 3:2 complex formed with CB[8]. These cathodic shifts support the conclusion that the viologen units are overall more difficult to reduce in the 3:2 complex than in the free guest, which is in agreement with the proposed complex featuring half of the V^{2+} units interacting with P_i donors. More detailed analyses focusing on the first reduction also confirmed that all the viologen units in CB[8]$_3^{\bullet}$(**V^{2+}P-A-PV^{2+}**-$(OMe)_2)_2$ are not in the same chemical environment, as clearly seen on the CV curve recorded at 100 mV.s^{-1} through the observation of a very broad wave featured by a shoulder at ca −0.35 V. Then, the large increase of about 350 mV in the stability domain of the bisradical **V$^{+\bullet}$P-A-PV$^{+\bullet}$**-$(OMe)_2$ ($\Delta Ep = E_{p2}$-E_{p1}) under the effect of its insertion in CB[8] suggests that the reduced complex CB[8]$_3^{\bullet}$(**V$^{+\bullet}$P-A-PV$^{+\bullet}$**-$(OMe)_2)_2$ undergoes at the CV time scale a *dissociation* driven by the stabilization of the bisradical **V$^{+\bullet}$P-A-PV$^{+\bullet}$**-$(OMe)_2$ as one of the intermolecular 2:2 π-dimer complexes shown in Figure 8, featuring viologen-based π-dimers[26] at both ends of the guests and two CB[8] hosts located on proximal or distal stations. The existence of electron-triggered reorganization processes yielding such discrete intermolecular π dimer complexes was further demonstrated by absorption spectroscopy measurements conducted after chemical reduction of the 3:2 complex CB[8]$_3^{\bullet}$(**V^{2+}P-A-PV^{2+}**-$(OMe)_2)_2$ or of the free guest **V^{2+}P-A-PV^{2+}**-$(OMe)_2$ used as a reference.

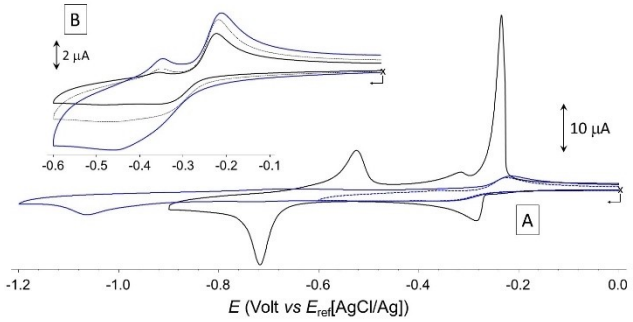

Figure 7. A) Voltamperometric curves recorded at 25 mV.s^{-1} for aqueous solutions of **VP-A-PV**-$(OMe)_2$ (1×10^{-3} M + 0.1 M LiCl) before (black line) and after (blue line) addition of 1.5 molar equiv. of CB[8]. B) Focus on the [−0.1 to −0.6 V] potential window, with CV curves recorded at 25 (full black line); 50 (dashed black line, and 100 (full blue line) mV.s^{-1} (vitreous carbon working electrode Ø = 3 mm).

As can be seen in Figure 9a, the addition of an excess of sodium dithionite to an oxygen-free aqueous solution of **V^{2+}P-A-PV^{2+}**-$(OMe)_2$ led to the development of i) an intense signal in the visible range showing shoulders at 500, 600 and 680 nm attributed to the free radical V$^{+\bullet}$[27] of **V$^{+\bullet}$P-A-PV$^{+\bullet}$**$^-$-$(OMe)_2$ and of ii) a very broad band extending from 800 to 1500 nm attributed to the formation of a mixture of intermolecular π-dimerized oligomers.[28]

Then, the chemical reduction of the 3:2 complex CB[8]$_3^{\bullet}$(**V^{2+}P-A-PV^{2+}**-$(OMe)_2)_2$ carried out in the same experimental conditions conversely led to different spectra (Figure 9b), including maxima at 608 and 963 nm which are fingerprint data supporting the formation of a discrete π dimer complex stabilized by CB[8] rings.[28a–c,29] Taken together, the electrochemical data recorded after addition of 1.5 molar equiv. of CB[8] are thus consistent with the formation of the proposed 3:2 complex. The main evidence

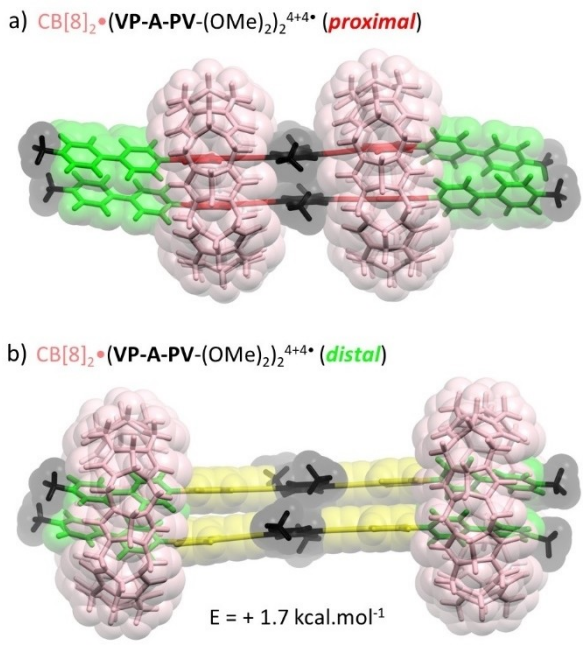

Figure 8. Lowest energy structures (DFT with dispersion) of two different pi-dimer 2:2 complexes with the general formula $CB[8]_2^{\bullet}(V^{+\bullet}$**P-A-**$PV^{+\bullet}$-$(OMe)_2)_2$ showing CB[8] hosts located on a) proximal or b) distal stations.

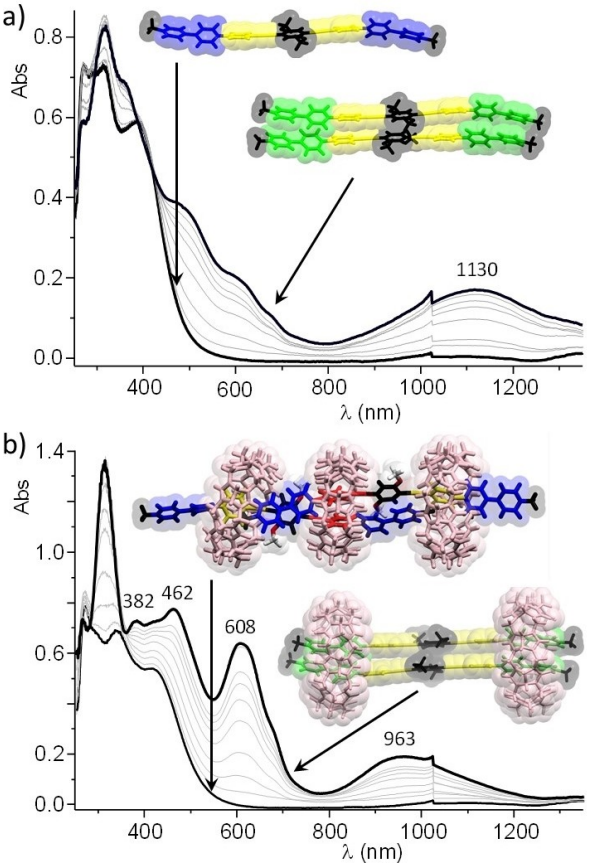

Figure 9. UV/Vis NIR absorption spectra recorded over time (1 spectrum/second) after the addition of excess $Na_2S_2O_4$ to an aqueous solution (1×10^{-3} M + 0.1 M LiCl) of a) **VP-A-PV**-$(OMe)_2$ and b) **VP-A-PV**-$(OMe)_2$ + 1.5 molar equiv. of CB[8] (l = 0.5 mm; only one 2:2 complex shown, for clarity).

being i) the loss in current intensity due to the formation of a large complex with lower diffusion properties than those of the free guest, ii) the observation of a broad reduction wave with shoulder suggesting the existence of different chemical environments for the four viologen units involved in the 3:2 complex and iii) the negative shift of the first reduction potential upon complexation, suggesting the association of the viologen units with electron rich stations. Then, the electron-triggered dissociation of the 3:2 complex affording the discrete π dimerized 2:2 complex $CB[8]_2^{\bullet}$(**VP-A-PV**-$(OMe)_2)_2^{4+4\bullet}$ was first revealed at the CV timescale by a very large cathodic shift of the second reduction wave and further confirmed by the observation of a diagnostic signal in the visible to near-infrared range. Our findings are conceptually summarized in Figure 10.

The masterpieces of these assemblies are the host:guest 1:2 complexes. CB[8] "*supramolecularly clicks*"[30] two molecules of **VP-A-PV** *by a new phenylenealkyne motif*, thereby providing a new platform from which several parameters could be explored toward the formation of larger 3:2 complexes (internal dynamics, *proximal* versus *distal* binding, effect of guest side-chains, host self-sorting, and effects of external stimuli).

Conclusion

A series of simple and symmetric guest molecules showed a surprisingly rich scenario of CB[*n*] binding in water. With a linear guest design featuring two mutually exclusive stations for CB[8] on *one* side of a guest (impossible to dock two CB[*n*]s on adjacent V and P stations),[16] but "compatible" stations on *two* guests, 3:2 host:guest complexes could be built displaying tunable modularity. A key parameter is probably the trend for this class of guests to include pairwise in a first CB[8] such as placing two phenylene-ethynylene (P_1) stations in the host cavity (a central {CB[8]•*P*•*P*} recognition motif), electrostatic repulsion between neighbouring viologen units probably playing a role in this arrangement (staggered threads in CB[8]). In most 3:2 complexes, two N^+-Me groups additionally co-include with the guests P_2 stations in two *proximal* peripheral CB[8], avoiding further host:guest assembly and supramolecular polymerization.[10a] Peripheral host binding appeared to considerably rigidify the whole 3:2 complexes, drastically reducing host and guest translational movements, in turn impacting the rotation of P_1 stations. This type of translational-rotational coupling between the host and the guest dynamics is unprecedented to our knowledge in large host:guest complexes in water. The role of the guest interfacial domain connecting subdomains A and B was explored toward understanding its impact in the apparent desymmetrization triggered by the initial binding event, the first binding on P_1 stations leaving identical P_2 stations, free.

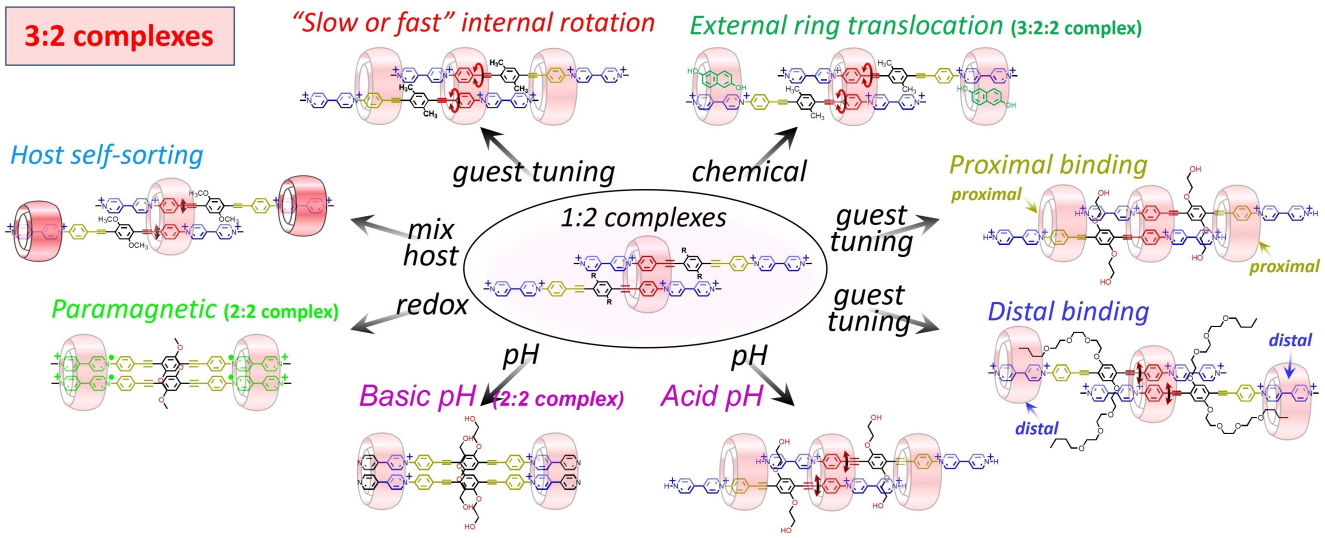

Figure 10. Schematic illustration showing the common (*central*) structural motif and the modular host:guest 3:2 complexes obtained mainly with CB[8].

With longer side-arms carrying hydrophobic extremities on VP-A-PV, consistent CB[8] binding was observed on P_1 stations but the 2 peripheral CB[8] were found to sit on *distal* V_2 stations, co-including one butyl group each. The rigidified 3:2 complex also showed rotation of the central, included P_1 stations, largely inhibited at room temperature. By taking advantage of the better affinity of CB[7] for the *distal* (viologen) stations, we could prepare mixed CB[8]:CB[7] complexes from the same CB[8]-P_1-P_1 core motif but with two CB[7]-V_2 recognition motifs, so placing another kind of macrocycle on *distal* stations. By using 2,6-dihydroxynaphthalene, we could also translocate two peripheral CB[8] from *proximal* to *distal* stations, keeping the initial architecture of the 3:2 host:guest complex (which transformed into a 3:2:2 host:guest:guest complex). Finally, the redox stimulus (reduction) was shown to transform 3:2 complexes into paramagnetic 2:2 complexes, and pH changes on a 2:2 complex of an analogue of VP-A-PV enabled access to a new 3:2 complex. These examples unambiguously demonstrate the potential of CB[*n*] macrocycles for the construction of sophisticated oligomeric assemblies in water. The present design based on rigid scaffolds is not limited to linear guest molecules and could in principle deliver a myriad of new supramolecular oligomers (curved or cyclic) with emergent properties using CB[8] in water.

Supporting Information

Details of chemical syntheses, characterizations, NMR, crystallization, ITC and theoretical calculations. Additional NMR spectra are also provided. The authors have cited additional references within the Supporting Information.[31–40]

Acknowledgements

CNRS and Aix-Marseille University are acknowledged for continuous support. Financial support from the IR-RMN-THC Fr3050 CNRS is gratefully acknowledged for experiments at 800 MHz and Mrs Cecile Chamignon as well for recording the corresponding spectra. This work received support from the French government under the France 2030 investment plan, as part of the Initiative d'Excellence d'Aix-Marseille Université - A*MIDEX." (AMX-20-IET-015). CB and DB wish to thank the French National Research Agency (ANR) for funding ANR-CE06-0020-01 (ANGEL) and ANR-22-CE07-0025 (STARGATE) as well as the "Mission pour les initiatives transverses et interdisciplinaires" MITI CNRS (Auto-organisation AAP 2020).

Conflict of Interest

The authors declare no conflict of interest.

Data Availability Statement

The data that support the findings of this study are available in the supplementary material of this article.

Keywords: Complexes · Cucurbituril · Stimulus · Supramolecular · Viologen

[1] a) L. Zhou, L. A. Sazanov, *Science* **2019**, *365*, eaaw9144; b) J. B. Rafferty, S. E. Sedelnikova, D. Hargreaves, P. J. Artymiuk, P. J. Baker, G. J. Sharples, A. A. Mahdi, R. G. Lloyd, D. W. Rice, *Science* **1996**, *274*, 415–421; c) R. H. P. Law, N. Lukoyanova, I. Voskoboinik, T. T. Caradoc-Davies, K. Baran, M. A. Dunstone, M. E. D'Angelo, E. V. Orlova, F.

Coulibaly, S. Verschoor, K. A. Browne, A. Ciccone, M. J. Kuiper, P. I. Bird, J. A. Trapani, H. R. Saibil, J. C. Whisstock, *Nature* **2010**, *468*, 447–451.
[2] R. M. Walsh, Jr, S.-H. Roh, A. Gharpure, C. L. Morales-Perez, J. Teng, R. E. Hibbs, *Nature* **2018**, *557*, 261–265.
[3] C. Labarca, M. W. Nowak, H. Zhang, L. Tang, P. Deshpande, H. A. Lester, *Nature* **1995**, *376*, 514–516.
[4] a) W. Liu, S. Bobbala, C. L. Stern, J. E. Hornick, Y. Liu, A. E. Enciso, E. A. Scott, J. F. Stoddart, *J. Am. Chem. Soc.* **2020**, *142*, 3165–3173; b) L. Cao, M. Sekutor, P. Y. Zavalij, K. Mlinaric-Majerski, R. Glaser, L. Isaacs, *Angew. Chem. Int. Ed.* **2014**, *53*, 988–993; c) Y. Liu, W. Zhao, C.-H. Chen, A. H. Flood, *Science* **2019**, *365*, 159–161; d) Q. He, P. Tu, J. L. Sessler, *Chem* **2018**, *4*, 46–93; e) M. Nilam, S. Karmacharya, W. M. Nau, A. Hennig, *Angew. Chem. Int. Ed.* **2022**, *61*, e202207950; f) M. Nilam, S. Collin, S. Karmacharya, A. Hennig, W. M. Nau, *ACS Sens.* **2021**, *6*, 175–182; g) A. Barba-Bon, Y.-C. Pan, F. Biedermann, D.-S. Guo, W. M. Nau, A. Hennig, *J. Am. Chem. Soc.* **2019**, *141*, 20137–20145.
[5] a) Y. Qiu, B. Song, C. Pezzato, D. Shen, W. Liu, L. Zhang, Y. Feng, Q.-H. Guo, K. Cai, W. Li, H. Chen, M. T. Nguyen, Y. Shi, C. Cheng, R. D. Astumian, X. Li, J. F. Stoddart, *Science* **2020**, *368*, 1247–1253; b) J. M. C. A. Kerckhoffs, F. W. B. van Leeuwen, A. L. Spek, K. Kooijman, M. Crego-Calama, D. N. Reinhoudt, *Angew. Chem. Int. Ed.* **2003**, *42*, 5717–5722; c) F. Liu, S. Chowdhury, R. Rosas, V. Monnier, L. Charles, H. Karoui, D. Gigmes, O. Ouari, F. Chevallier, C. Bucher, A. Kermagoret, S. Liu, D. Bardelang, *Org. Lett.* **2021**, *23*, 5283–5287.
[6] a) L. Melidis, H. J. Hill, N. J. Coltman, S. P. Davies, K. Winczura, T. Chauhan, J. S. Craig, A. Garai, C. A. J. Hooper, R. T. Egan, J. A. McKeating, N. J. Hodges, Z. Stamataki, P. Grzechnik, M. J. Hannon, *Angew. Chem. Int. Ed.* **2021**, *60*, 18144–18151; b) Y.-D. Yang, X.-L. Chen, J. L. Sessler, H.-Y. Gong, *J. Am. Chem. Soc.* **2021**, *143*, 2315–2324; c) H. Wu, Y. Wang, L. O. Jones, W. Liu, B. Song, Y. Cui, K. Cai, L. Zhang, D. Shen, X.-Y. Chen, Y. Jiao, C. L. Stern, X. Li, G. C. Schatz, J. F. Stoddart, *J. Am. Chem. Soc.* **2020**, *142*, 16849–16860; d) H.-Q. Peng, W. Zhu, W.-J. Guo, Q. Li, S. Ma, C. Bucher, B. Liu, X. Ji, F. Huang, J. L. Sessler, *Prog. Polym. Sci.* **2023**, *137*, 101635.
[7] a) M. Tominaga, K. Suzuki, M. Kawano, T. Kusukawa, T. Ozeki, S. Shakamoto, K. Yamaguchi, M. Fujita, *Angew. Chem. Int. Ed.* **2004**, *43*, 5621–5625; b) C. T. McTernan, J. A. Davies, J. R. Nitschke, *Chem. Rev.* **2022**, *122*, 10393–10437; c) S. Sudan, F. Fadaei-Tirani, R. Scopelliti, K. E. Ebbert, G. H. Clever, K. Severin, *Angew. Chem. Int. Ed.* **2022**, *61*, e202201823; d) J.-N. Rebilly, B. Colasson, O. Bistri, D. Over, O. Reinaud, *Chem. Soc. Rev.* **2015**, *44*, 467–489.
[8] a) J. M. C. A. Kerckhoffs, M. G. J. Ten Cate, M. A. Mateos-Timoneda, F. W. B. Van Leeuwen, B. Snellink-Rüel, A. L. Spek, H. Kooijman, M. Crego-Calama, D. N. Reinhoudt, *J. Am. Chem. Soc.* **2005**, *127*, 12697–12708; b) S. J. Dalgarno, S. A. Tucker, D. B. Bassil, J. L. Atwood, *Science* **2005**, *309*, 2037–2039; c) M. C. O'Sullivan, J. K. Sprafke, D. V. Kondratuk, C. Rinfray, T. D. W. Claridge, A. Saywell, M. O. Blunt, J. N. O'Shea, P. H. Beton, M. Malfois, H. L. Anderson, *Nature* **2011**, *469*, 72–75; d) T. Zhang, L. Le Corre, O. Reinaud, B. Colasson, *Chem. Eur. J.* **2021**, *27*, 434–443.
[9] a) J. Lagona, P. Mukhopadhyay, S. Chakrabarti, L. Isaacs, *Angew. Chem. Int. Ed.* **2005**, *44*, 4844–4870; b) S. J. Barrow, S. Kasera, M. J. Rowland, J. del Barrio, O. A. Scherman, *Chem. Rev.* **2015**, *115*, 12320–12406; c) J. W. Lee, S. Samal, N. Selvapalam, H.-J. Kim, K. Kim, *Acc. Chem. Res.* **2003**, *36*, 621–630; d) E. Masson, X. Ling, R. Joseph, L. Kyeremeh-Mensah, X. Lu, *RSC Adv.* **2012**, *2*, 1213–1247; e) K. I. Assaf, W. M. Nau, *Chem. Soc. Rev.* **2015**, *44*, 394–418; f) M. A. Alnajjar, W. M. Nau, A. Hennig, *Org. Biomol. Chem.* **2021**, *19*, 8521–8529.
[10] a) X. Yang, R. Wang, A. Kermagoret, D. Bardelang, *Angew. Chem. Int. Ed.* **2020**, *59*, 21280–21292; b) G. Wu, Z. Huang, O. A. Scherman, *Angew. Chem. Int. Ed.* **2020**, *59*, 15963–15967; c) S. Murkli, J. N. McNeill, L. Isaacs, *Supramol. Chem.* **2019**, *31*, 150–158; d) M. Raeisi, K. Kotturi, I. del Valle, J. Schulz, P. Dornblut, E. Masson, *J. Am. Chem. Soc.* **2018**, *140*, 3371–3377.
[11] a) L. Cera, C. A. Schalley, *Chem. Sci.* **2014**, *5*, 2560–2567; b) R. Joseph, A. Nkrumah, R. J. Clark, E. Masson, *J. Am. Chem. Soc.* **2014**, *136*, 6602–6607; c) Q. Qi, B. Yang, C.-G. Xi, X. Yang, D.-W. Zhang, S. Liu, Z.-T. Li, *ChemistrySelect* **2016**, *1*, 6792–6796; d) Q. Li, J.-D. Sun, B. Yang, H. Wang, D.-W. Zhang, D. Ma, Z.-T. Li, *Chin. Chem. Lett.* **2022**, *33*, 1988–1992.
[12] a) Y. Xu, M. Guo, X. Li, A. Malkovskiy, C. Wesdemiotis, Y. Pang, *Chem. Commun.* **2011**, *47*, 8883–8885; b) J. del Barrio, P. N. Horton, D. Lairez, G. O. Lloyd, C. Toprakcioglu, O. A. Scherman, *J. Am. Chem. Soc.* **2013**, *135*, 11760–11763; c) X. Xiao, R.-L. Lin, L.-M. Zheng, W.-Q. Sun, Z. Tao, S.-F. Xue, Q.-J. Zhu, J.-X. Liu, *RSC Adv.* **2014**, *4*, 53665–53668; d) P.-Q. Zhang, Q. Li, Z.-K. Wang, Q.-X. Tang, P.-P. Liu, W.-H. Li, G.-Y. Yang, B. Yang, D. Ma, Z.-T. Li, *Chin. Chem. Lett.* **2023**, *34*, 107632.
[13] a) N. Barooah, R. Khurana, J. Mohanty, A. C. Bhasikuttan, *ChemistrySelect* **2017**, *2*, 7387–7393; b) N. Barooah, J. Mohanty, A. C. Bhasikuttan, *Chem. Commun.* **2015**, *51*, 13225–13228; c) Z.-J. Zhang, H.-Y. Zhang, L. Chen, Y. Liu, *J. Org. Chem.* **2011**, *76*, 8270–8276; d) E. V. Peresypkina, V. P. Fedin, V. Maurel, A. Grand, P. Rey, K. E. Vostrikova, *Chem. Eur. J.* **2010**, *16*, 12481–12487; e) S. Andersson, D. Zou, R. Zhang, S. Sun, L. Sun, *Org. Biomol. Chem.* **2009**, *7*, 3605–3609; f) X. Zhang, T. Sun, X.-L. Ni, *Org. Chem. Front.* **2021**, *8*, 32–38; g) M.-X. Yang, Y. Luo, W. Zhang, W.-h. Lin, J. He, P.-h. Shan, Z. Tao, X. Xiao, *Chem. Asian J.* **2022**, *17*, e202200378; h) N. Hickey, B. Medagli, A. Pedrini, R. Pinalli, E. Dalcanale, S. Geremia, *Cryst. Growth Des.* **2021**, *21*, 3650–3655; i) G. Wu, I. Szabo, E. Rosta, O. A. Scherman, *Chem. Commun.* **2019**, *55*, 13227–13230; j) W. Jiang, Q. Wang, I. Linder, F. Klautzsch, C. A. Schalley, *Chem. Eur. J.* **2011**, *17*, 2344–2348; k) C. P. Carvalho, Z. Domínguez, C. Domínguez, J. F. Arteaga, U. Pischel, H. S. El-Sheshtawy, J. P. D. Silva, *ChemistryOpen* **2017**, *6*, 288–294.
[14] a) W. Ong, M. Gómez-Kaifer, A. E. Kaifer, *Org. Lett.* **2002**, *4*, 1791–1794; b) H.-J. Kim, W. S. Jeon, Y. H. Ko, K. Kim, *Proc. Natl. Acad. Sci. USA* **2002**, *99*, 5007–5011; c) X. Yang, Q. Cheng, V. Monnier, L. Charles, H. Karoui, O. Ouari, D. Gigmes, R. Wang, A. Kermagoret, D. Bardelang, *Angew. Chem. Int. Ed.* **2021**, *60*, 6617–6623; d) H. Yin, Q. Cheng, R. Rosas, S. Viel, V. Monnier, L. Charles, D. Siri, D. Gigmes, O. Ouari, R. Wang, A. Kermagoret, D. Bardelang, *Chem. Eur. J.* **2019**, *25*, 12552–12559.
[15] a) S. Liu, C. Ruspic, P. Mukhopadhyay, S. Chakrabarti, P. Y. Zavalij, L. Isaacs, *J. Am. Chem. Soc.* **2005**, *127*, 15959–15967; b) S. K. Samanta, D. Moncelet, V. Briken, L. Isaacs, *J. Am. Chem. Soc.* **2016**, *138*, 14488–14496; c) L. C. Smith, D. G. Leach, B. E. Blaylock, O. A. Ali, A. R. Urbach, *J. Am. Chem. Soc.* **2015**, *137*, 3663–3669; d) G. A. Vincil, A. R. Urbach, *Supramol. Chem.* **2008**, *20*, 681–687.
[16] H. Yin, R. Rosas, D. Gigmes, O. Ouari, R. Wang, A. Kermagoret, D. Bardelang, *Org. Lett.* **2018**, *20*, 3187–3191.
[17] Deposition number 2182217 ($CB[8]_1$•(**VP-A-PV**-$(OMe)_2)_2$) contains the supplementary crystallographic data for this paper. These data are provided free of charge by the joint Cambridge Crystallographic Data Centre and Fachinformationszentrum Karlsruhe Access Structures service.
[18] S. Combes, K. T. Tran, M. M. Ayhan, H. Karoui, A. Rockenbauer, A. Tonetto, V. Monnier, L. Charles, R. Rosas, S.

Viel, D. Siri, P. Tordo, S. Clair, R. Wang, D. Bardelang, O. Ouari, *J. Am. Chem. Soc.* **2019**, *141*, 5897–5907.
[19] a) Y. Wu, G. Wang, Q. Li, J. Xiang, H. Jiang, Y. Wang, *Nat. Commun.* **2018**, *9*, 1953; b) C. Yu, L. Ma, J. He, J. Xiang, X. Deng, Y. Wang, X. Chen, H. Jiang, *J. Am. Chem. Soc.* **2016**, *138*, 15849–15852.
[20] a) G. Wu, Y. J. Bae, M. Olesińska, D. Antón-García, I. Szabó, E. Rosta, M. R. Wasielewski, O. A. Scherman, *Chem. Sci.* **2020**, *11*, 812–825; b) M. Olesińska, G. Wu, S. Gómez-Coca, D. Antón-García, I. Szabó, E. Rosta, O. A. Scherman, *Chem. Sci.* **2019**, *10*, 8806–8811.
[21] W. Xu, J. Kan, B. Yang, T. J. Prior, B. Bian, X. Xiao, Z. Tao, C. Redshaw, *Chem. Asian J.* **2019**, *14*, 235–242.
[22] a) K. Kotturi, E. Masson, *Chem. Eur. J.* **2018**, *24*, 8670–8678; b) H. Barbero, E. Masson, *Chem. Sci.* **2021**, *12*, 9962–9968.
[23] a) H.-J. Kim, J. Heo, W. S. Jeon, E. Lee, J. Kim, S. Sakamoto, K. Yamaguchi, K. Kim, *Angew. Chem. Int. Ed.* **2001**, *40*, 1526–1529; b) Y. H. Ko, E. Kim, I. Hwang, K. Kim, *Chem. Commun.* **2007**, 1305–1315.
[24] E. Pazos, P. Novo, C. Peinador, A. E. Kaifer, M. D. García, *Angew. Chem. Int. Ed.* **2019**, *58*, 403–416.
[25] a) Z.-J. Zhang, Y.-M. Zhang, Y. Liu, *J. Org. Chem.* **2011**, *76*, 4682–4685; b) K.-D. Zhang, J. Tian, D. Hanifi, Y. Zhang, A. C.-H. Sue, T.-Y. Zhou, L. Zhang, X. Zhao, Y. Liu, Z.-T. Li, *J. Am. Chem. Soc.* **2013**, *135*, 17913–17918; c) C. Kahlfuss, E. Metay, M.-C. Duclos, M. Lemaire, A. Milet, E. Saint-Aman, C. Bucher, *Chem. Eur. J.* **2015**, *21*, 2090–2106.
[26] N. Le Poul, B. Colasson, *ChemElectroChem* **2015**, *2*, 475–496.
[27] C. Kahlfuss, S. Chowdhury, A. F. Carreira, R. Grüber, E. Dumont, D. Frath, F. Chevallier, A. Eric Saint, C. Bucher, *Inorg. Chem.* **2021**, *60*, 3543–3555.
[28] a) C. Kahlfuss, E. Saint-Aman, C. Bucher, in *Organic Redox Systems* (Ed.: T. Nishinaga), Wiley, Hoboken, **2016**, pp. 39–88; b) H. D. Correia, S. Chowdhury, A. P. Ramos, L. Guy, G. J.-F. Demets, C. Bucher, *Polym. Int.* **2019**, *64*, 572–588; c) K. Cai, L. Zhang, R. D. Astumian, J. F. Stoddart, *Nat. Chem. Rev.* **2021**, *5*, 447–465; d) D.-W. Zhang, J. Tian, L. Chen, L. Zhang, Z.-T. Li, *Chem. Asian J.* **2015**, *10*, 56–68.
[29] a) S. Al Shehimy, O. Baydoun, S. Denis-Quanquin, J.-C. Mulatier, L. Khrouz, D. Frath, E. Dumont, M. Murugesu, F. Chevallier, C. Bucher, *J. Am. Chem. Soc.* **2022**, *144*, 17955–17965; b) C. Kahlfuss, S. Denis-Quanquin, N. Calin, E. Dumont, M. Garavelli, G. Royal, S. Cobo, E. Saint-Aman, C. Bucher, *J. Am. Chem. Soc.* **2016**, *138*, 15234–15242; c) L. Zhang, T.-Y. Zhou, J. Tian, H. Wang, D.-W. Zhang, X. Zhao, Y. Liu, Z.-T. Li, *Polym. Chem.* **2014**, *5*, 4715–4721.
[30] a) J. W. Lee, S. C. Hain, J. H. Kim, Y. H. Ko, K. Kim, *Bull. Korean Chem. Soc.* **2007**, *28*, 1837–1840; b) W. Wang, A. E. Kaifer, *Angew. Chem. Int. Ed.* **2006**, *45*, 7042–7046.
[31] D. Bardelang, K. A. Udachin, D. M. Leek, J. C. Margeson, G. Chan, C. I. Ratcliffe, J. A. Ripmeester, *Cryst. Growth Des.* **2011**, *11*, 5598–5614.
[32] O. V. Dolomanov, L. J. Bourhis, R. J. Gildea, J. A. K. Howard, H. Puschmann, *J. Appl. Crystallogr.* **2009**, *42*, 339–341.
[33] G. M. Sheldrick, *Acta Crystallogr. Sect. A* **2015**, *71*, 3–8.
[34] G. M. Sheldrick, *Acta Crystallogr. Sect. C* **2015**, *71*, 3–8.
[35] Gaussian 16, Revision A.03, M. J. Frisch, G. W. Trucks, H. B. Schlegel, G. E. Scuseria, M. A. Robb, J. R. Cheeseman, G. Scalmani, V. Barone, G. A. Petersson, H. Nakatsuji, X. Li, M. Caricato, A. V. Marenich, J. Bloino, B. G. Janesko, R. Gomperts, B. Mennucci, H. P. Hratchian, J. V. Ortiz, A. F. Izmaylov, J. L. Sonnenberg, D. Williams-Young, F. Ding, F. Lipparini, F. Egidi, J. Goings, B. Peng, A. Petrone, T. Henderson, D. Ranasinghe, V. G. Zakrzewski, J. Gao, N. Rega, G. Zheng, W. Liang, M. Hada, M. Ehara, K. Toyota, R. Fukuda, J. Hasegawa, M. Ishida, T. Nakajima, Y. Honda, O. Kitao, H. Nakai, T. Vreven, K. Throssell, J. A. Montgomery, Jr, J. E. Peralta, F. Ogliaro, M. J. Bearpark, J. J. Heyd, E. N. Brothers, K. N. Kudin, V. N. Staroverov, T. A. Keith, R. Kobayashi, J. Normand, K. Raghavachari, A. P. Rendell, J. C. Burant, S. S. Iyengar, J. Tomasi, M. Cossi, J. M. Millam, M. Klene, C. Adamo, R. Cammi, J. W. Ochterski, R. L. Martin, K. Morokuma, O. Farkas, J. B. Foresman, D. J. Fox, Gaussian, Inc, Wallingford CT, **2016**.
[36] M. J. Abraham, T. Murtola, R. Schulz, S. Páll, J. C. Smith, B. Hess, E. Lindahl, GROMACS: High performance molecular simulations through multi-level parallelism from laptops to supercomputers, SoftwareX 1 (**2015**) pp. 19–25.
[37] S. Grunder, R. Huber, V. Horhoiu, M. T. Gonzalez, C. Schönenberger, M. Calame, M. Mayor, *J. Org. Chem.* **2007**, *72*, 8337–8344.
[38] M. B. Ramey, Hille, M. F. Rubner, C. Tan, K. S. Schanze, J. R. Reynolds, *Macromolecules* **2005**, *38*, 234–243.
[39] M. T. González, X. Zhao, D. Z. Manrique, D. Miguel, E. Leary, M. Gulcur, A. S. Batsanov, G. Rubio-Bollinger, C. J. Lambert, M. R. Bryce, N. Agraït, *J. Phys. Chem. C* **2014**, *118*, 21655–21662.
[40] Q. Li, Y.-Q. Zhang, Q.-J. Zhu, S.-F. Xue, Z. Tao, X. Xiao, *Chem. Asian J.* **2015**, *10*, 1159–1164.

Manuscript received: October 22, 2023
Accepted manuscript online: November 27, 2023
Version of record online: December 7, 2023